The Kennesaw Journal of Undergraduate Research

Volume 11 | Issue 1 Article 7

2024

Winglet Vortex Optimization

Adeel Khalid
Kennesaw State University, akhalid2@kennesaw.edu

Anthony Gutierrez
Kennesaw State University, mgutie28@students.kennesaw.edu

Follow this and additional works at: https://digitalcommons.kennesaw.edu/kjur

 Part of the Aerodynamics and Fluid Mechanics Commons

Recommended Citation

Khalid, Adeel and Gutierrez, Anthony (2024) "Winglet Vortex Optimization," *The Kennesaw Journal of Undergraduate Research*: Vol. 11: Iss. 1, Article 7.
DOI: https://doi.org/10.62915/2474-4921.1275
Available at: https://digitalcommons.kennesaw.edu/kjur/vol11/iss1/7

This Article is brought to you for free and open access by the Active Journals at DigitalCommons@Kennesaw State University. It has been accepted for inclusion in The Kennesaw Journal of Undergraduate Research by an authorized editor of DigitalCommons@Kennesaw State University. For more information, please contact digitalcommons@kennesaw.edu.

Winglet Vortex Optimization

Anthony Gutierrez
Undergraduate Student, Kennesaw State University, Marietta, Georgia, 30060, United States of America

Adeel Khalid, Ph.D.

Professor, Kennesaw State University, Marietta, Georgia, 30060, United State of America

ABSTRACT

The objective of this research is to determine the effect on aerodynamic performance due to changes of winglet design variables of the Boeing 737-700 aircraft. The various winglet types studied in this research include the blended, canted, wingtip fence and split scimitar. The variables include height, sweep angle, taper ratio, and inclination angle. These variables are altered in 5% increments from -15% to +15% of their original baseline values. Each altered winglet design only changes one variable at a time while keeping all other variables constant. The altered models are compared to the original by finding the aerodynamic efficiency through Computational Fluid Dynamics in SolidWorks. For this study, aerodynamic efficiency is defined as lift to drag ratio generated by the isolated wing coupled with the corresponding winglet design. For empirical analysis, the optimized winglets are scaled down, 3D printed, and tested for their aerodynamic efficiency in the AEROLAB Educational Wind Tunnel. This study concludes that the blended winglet reaches peak aerodynamic efficiency with an increase to the sweep angle of +10% of the original baseline blended winglet value found on the B737-700 winglet. Additionally, aerodynamic efficiency of the canted winglet peaks at an inclination angle of 45 degrees. The wingtip fence winglet derived from the Airbus A320 performed the best at its baseline values. Lastly, the split scimitar winglet performs best with the lower member as the full cord length and scaled down to 50% of the top member. This study focuses on the relative changes of each winglet and its changes to aerodynamic efficiency.

NOMENCLATURE

λ - The taper ratio is the ratio of the equivalent length of the winglet tip to the equivalent length of the winglet root

ϕ - Inclination angle: the angle between the winglet and the horizontal, a 90-degree angle while a 0-degree angle is a winglet on the wing plane.

γ - Sweep Angle: the equivalent angle between the horizontal axis and the inclined line leading to the leading edge of the winglet tip.

C_d - Drag coefficient

D - Drag

d - Depth (m): measure of the winglet extruding members below the mean cord line

L - Lift

L/D - Aerodynamic Efficiency (Lift to Drag ratio)

c - chord

h - Height (m): measure of the winglet tip from the mean cord line

ρ - Density

N

V

AOA

CFD

OEM

I.

Winglets

The

II.

A.

No wing with no winglet has an abrupt end to the wing. There is no additional geometry at the end of the wing. Some examples of planes with no winglets include early versions of the B737 such as the -100 and -300.

Figure

B.

Airbus

Figure

C.

The

Figure

D.

The

Figure

E.

This

Figure

These

For

III.

The assumptions in this experiment

To simplify the following CFD
The

IV.

A.

At cruise, an aircraft is in steady level flight conditions; the generated lift from the aircraft is equal to the weight of the aircraft as the aircraft maintains altitude. This flight condition is where airliners are optimized for efficiency due to length of time spent at cruise conditions. $\mathbf{Ltotal} = \mathbf{W} = \mathbf{m} * \mathbf{g}$ converts the calculated lift into the Si unit for force, newton, N. Also in cruise conditions, thrust is equal to drag as the aircraft maintains constant velocity. In $\boldsymbol{Lwing} = \frac{\mathbf{1}}{\mathbf{2}} * \boldsymbol{L\_total}$, the lift generated for each wing can be found using the total from Equation 1. With the known cruise thrust, the drag could be calculated for the entire aircraft as shown in $\boldsymbol{T}=\boldsymbol{D}$.

$$\mathbf{L_{total}} = \mathbf{W} = \mathbf{m} * \mathbf{g} \quad (1)$$

$$\boldsymbol{L_{wing}} = \frac{\mathbf{1}}{\mathbf{2}} * \boldsymbol{L\_total} \quad (2)$$

$$\boldsymbol{T} = \boldsymbol{D} \quad (3)$$

B.

With the total drag now known, the drag components of the fuselage and 2 nacelles can be calculated using $\boldsymbol{D}=\boldsymbol{1}\square\boldsymbol{2}\square * \boldsymbol{\rho} *$

$V^2 * C_d * S$. The fuselage and nacelles are treated as a circular flat plate for this experiment. In $Dwings = T_{Engine} - (D_{fuselage} + 2 * D_{nacelle})$, the sum of the drag totals of the fuselage and nacelles are subtracted from the engine cruise conditions to find the drag from the wings. $Dwing = \frac{1}{2} * D\_wings$ splits the total from Equation 4 to find the total drag for each wing.

$$D = \frac{1}{2} * \rho * V^2 * C_d * S \quad (4)$$

$$D_{wings} = T_{Engine} - (D_{fuselage} + 2 * D_{nacelle}) \quad (5)$$

$$D_{wing} = \frac{1}{2} * D\_wings \quad (6)$$

With the calculated lift and drag per wing, a L/D can now be found in $LD = \frac{L_{wing}}{D_{wing}}$.

$$\frac{L}{D} = \frac{L_{wing}}{D_{wing}} \quad (7)$$

Table 1. Baseline boundary conditions

Variable	Description	Value
W	Weight during cruise	64,342 kg
g	Gravity constant	9.81 m/s^2
T	Thrust during cruise	215.3 kN
ρ	Air density at 12.5 km	0.31194 N/m^2
V	Cruise velocity	237 m/s
C_d	Flat circular plate coefficient of drag	1.12
S_fuselage	Cross sectional area of fuselage	11.1 m^2

In Table 1, all the assumed and known variables are found in the Boeing 737 Detailed Technical Data sheet [8] and the CFM56-7 data sheet [14]. Using Equation 1, the total lift needed to maintain steady flight during cruise conditions is 631.2 kN. This means each wing will be roughly responsible for 315.6 kN using Equation 2. The thrust during the cruise segment will be equal to the drag experienced by the aircraft and is found to be 215.3 kN. Using Equation 4, the drag component of the fuselage is found. For this, the diameter of the fuselage is 3.76 meters. This value is used to find the frontal area and is assumed to be flat circular plates for the simplicity of this study. Equation 5 takes the drag component of the fuselage and subtracts that from the thrust/drag in Equation 3 to find the total drag of the two wings. The total drag of the two wings is found to be 106.35 kN and Equation 6 finds the drag component per wing, 53.17 kN. Using Equation 7, the aerodynamic efficiency of a B737-700 wing is found to be 5.93.

Table 1. Baseline B737-700 cruise conditions

Component	Value	
Total Lift= Cruise Weight	64.28 kN	(eqn 1)
Lift per Wing	32.14 kN	(eqn 2)
Thrust=Drag	215.3 kN	(eqn 3)
Fuselage Drag	108.94 kN	(eqn 4)
Total Engine Nacelle Drag	65.40 kN	(eqn 4)
Total Wing Drag	40.94 kN	(eqn 6)
Drag per Wing	20.47 kN	(eqn 7)
Aerodynamic Efficiency	**5.93**	(eqn 7)

To summarize the numerical set up, the empennage was ignored, fuselage provides negligible lift, and the fuselage and engine nacelles are analyzed as flat plates. The drag and lift components are isolated for the wing and the Boeing 737-700 original wing/winglet yields an aerodynamic efficiency of 5.93. This simplified numerical exercise is compared to the simulation value found in the next section.

V. EXPERIMENTAL SETUP

A. 3D Modeling

The Solidworks 3D modeling program is used to model the wing and winglet of the Boeing 737-700. The technical data used to model are found in the Boeing 737 detailed technical data [8], airfoil tools [17] and University of Illinois Urbana-Champaign airfoil data site [18]. Boeing aerodynamics designed and used 3 different airfoils for the b737 wing. The first is the root airfoil, (b737a-il), midspan airfoil (b737b-il), outboard and winglet airfoil (b737d-il). Using airfoil tools, the coordinates for each airfoil are imported into Solidworks at different drawings and planes. Then, these airfoil drawings are lofted into each other to create one smooth wing. The span of the wing measures 17.85 meters with a dihedral angle of about 15 degrees. **Error! Reference source not found.** displays the original B737-700 wing and winglet. For this study, the winglet is modified while the wing stays unchanged.

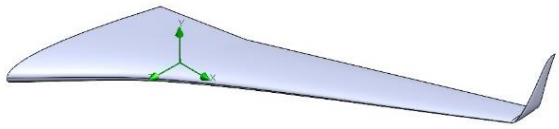

Figure 6. Boeing 737-700 (OEM)

B. Computational Fluid Dynamics (CFD)

Using Solidworks Flow Simulation, the computational domain of 4 times the greatest length in each of the X, Y and Z directions of the wing are used as seen in Figure 1. All CFD simulations are axis-symmetric analyses with vertical plane of the root of the wing. The Boeing 737-700 cruises at a speed of 237 m/s at an altitude of 40,000 ft (12,192 m) [8]. The corresponding atmospheric conditions on a standard day are shown in Table 2 and found in Appendix B of Aircraft Design: A conceptual Approach by D. Raymer [15]. The typical angle of attack (AOA) during cruise conditions is at +3 degrees. These conditions are used in Solidworks Flow Simulation to simulate the environmental conditions the wing will endure at 12,192 meters above sea level.

Table 2. CFD boundary conditions

Cruise Conditions/ Boundary Conditions	
Alt (m)	12,192
Density (kg/m^3)	0.31194
Pressure (N/m^2)	19,399
Temperature (k)	216.7
Speed (m/s)	237
AOA (degree)	3

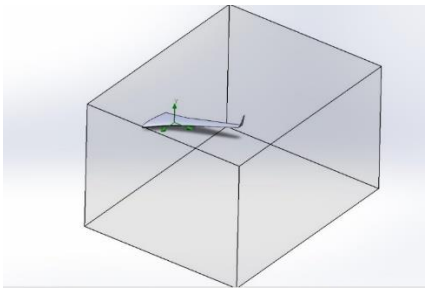

Figure 7. Computational domain

The goals of the Solidworks simulations are to calculate the force experienced by the wing in the Y and Z diction as seen in Figure 8. The Y diction force is the lifting force while the Z diction force is the drag force generated by the wing. Due to the number of simulations needed for this project. All solutions have an auto-generated medium level mesh. The time required for each simulation does not exceed 10 minutes. To validate the hand calculations the virtual wing tunnel test for the Original Boeing 737-700 Wing and winglet, are ran multiple times. With a total number of cells at about 433,000 cells the L/D ratio is found

to be 5.93. This experiment is repeatable and yields similar performance. The aerodynamic efficiency found in the simulation is slightly off from 3.42 but is within acceptable limits. This difference could be due to the assumptions taken for the numerical findings. The lift generated by the fuselage and empennage, skin friction, drag interference and parasitic drags are neglected. This means that the lift and drag components of the wing are higher and lower than expected, respectively. The original B737-700 aerodynamic efficiency of 5.93 will be the basis for all comparisons for all other winglets and configurations.

VI. WINGLETS

A. No Winglet

The OEM winglet of the Boeing 737-700 is a blended winglet. However, to test the effectiveness of the base winglet, a simulation is performed on just the wing. This wing is 17.65 m in span. In CFD, using the boundary conditions found in Table 3, the aerodynamic efficiency is found to be 3.17.

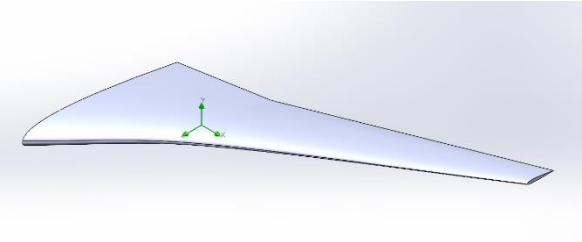

Figure 7. B737-700 Wing without a winglet

B. Blended Winglet

The OEM winglet on the Boeing 737-700 is a blended winglet. Through the hand calculations and assumptions made, the aerodynamic efficiency was calculated to be 5.93. Under the same boundary conditions in SolidWorks Flow Simulation, the aerodynamic efficiency is 3.45. These numbers do not agree because this experiment ignores the lift generated by the fuselage and empennage and only considers the pressure drag generated by the wing. However, when examining the winglet designs, an aerodynamic efficiency of 3.45 will be used as a baseline comparison.

The five variables that will be considered for the various winglet designs are the height, depth, sweep angle, taper ratio, and inclination angle. Figure 9 and Figure 10 display how the geometry for each parameter is set. A positive change in height means the winglet is taller than the original and a negative change in height means the winglet is shorter than the original. This is the same for taper ratio and sweep angle. For winglets that include a depth, the depth is the length of any member that protrudes below the wing while maintaining all other parameters. The inclination angle will vary from 0-90 degrees. A 0-degree inclination angle means the winglet is on the wing plane while a 90-degree inclination angle has the winglet perpendicular to the horizontal axis.

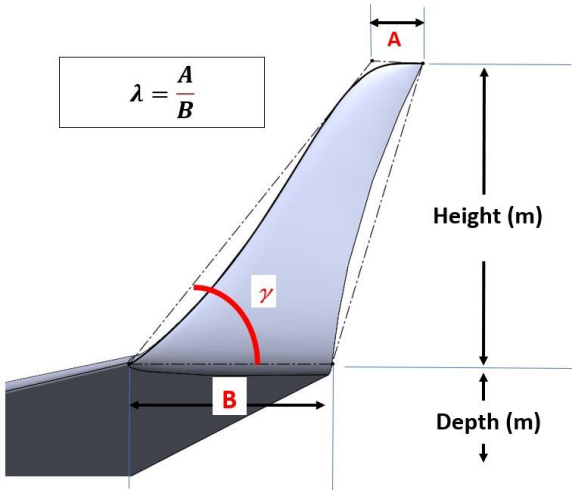

Figure 8. Blended winglet geometry 1

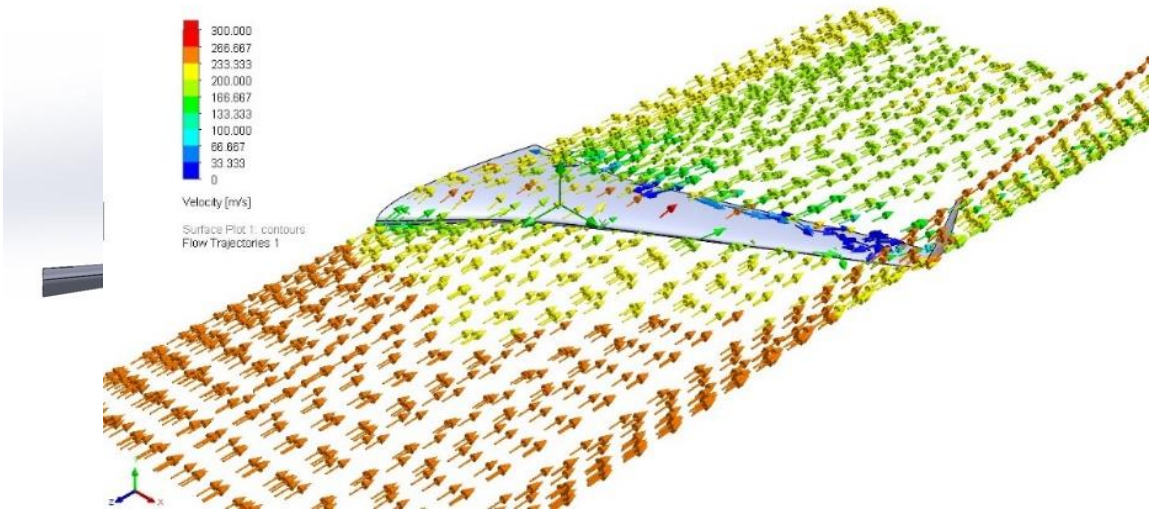

Figure 9. Blended winglet geometry 2

Figure 10. B737-700 OEM velocity profile

Table 3. Design of experiment table for blended winglet

	Parameter	-15%	-10%	-5%	Baseline	+5%	+10%	+15%
Blended Winglet	Height (m)	1.85	1.96	2.07	2.18	2.29	2.40	2.51
	Sweep Angle (degree)	43.58	46.15	48.71	51.28	53.84	56.40	58.97
	Taper Ratio	0.212	0.225	0.237	0.250	0.262	0.275	0.287
	Inclination Angle (degree)	15	30	45	90	75	60	-

Table 4. Blended winglet CFD results - L/D output in terms of % change

	Parameter	-15%	-10%	-5%	Baseline	+5%	+10%	+15%
Blended Winglet	Height (m)	+8.83%	+7.83%	+8.20%	L/D = 3.45	-1.76%	-0.06%	-2.90%
	Sweep Angle (degree)	-9.62%	-12.81%	-9.62%		+9.28%	+9.29%	+5.10%
	Taper Ratio	-7.81%	-4.76%	-7.81%		-5.72%	-5.74%	-9.71%
	Inclination Angle (degree)	15 deg	30 deg	45 deg		60 deg	75 deg	
		-6.39%	-5.78%	-2.18%		-4.18%	-4.19%	-

Error! Reference source not found. displays the data for each parameter. The baseline is the OEM B737-700, and each parameter is changed by 5% increments from -15% to +15% geometry except for the inclination angle. The inclination angle is changed by 15-degree increments starting at 15-degrees up to 90-degres. There is no depth data for the blended winglet as there are no members below the wing plane. For each parameter change, only that parameter will differ from the baseline while all other parameters stay consistent.

Error! Reference source not found. shows the velocity profile on the B737-700 OEM wing and winglet. The air flow is set to 237 m/s at a density of 19,399 Pa and a temperature of 216.7 k.

Table **4** shows the aerodynamic efficiency of all the winglet changes. The greatest aerodynamic efficiency in each parameter is -15% reduction in the height, +10% change is sweep angle, baseline taper ratio and baseline inclination.

Figure 11 displays the aerodynamic efficiency changes (L/D) compared to the baseline, the same data found in Table **4**. For any positive change in the aerodynamic efficiency, the data point is above the x axis and a negative change will be below the x axis.

For the height changes of the blended winglet baseline, the aerodynamic changes peak at the -15% height change of the winglet which generates a +8.83% increase in the aerodynamic efficiency. All 3 studies of decreasing the height of winglet yield positive changes to the aerodynamic efficiencies. Increasing the height of the winglet produces minor yet negative changes in L/D. Decreasing the height of an object such as a winglet would decrease the profile drag thus increasing L/D.

The baseline sweep angle of the winglet is 54.0 degrees, and this study looks at a sweep angle range from 45.9 to 62.1 degrees. By decreasing the sweep angle of the blended winglet, the aerodynamic efficiency decreases while increasing the sweep angle increases the aerodynamic efficiency. The 5% and 10% increase in sweep angle winglets both produce 9.28% and 9.29% increases in aerodynamic efficiency.

The taper ratio is the ratio of the equivalent length of the winglet tip to the cord length of the wing tip. The taper ratio of

the baseline winglet is 0.25. The changes of the taper ratio in this experiment for the blended winglet range from 0.2125 to 0.2875. All the changes in the taper ratio compared to the winglet, positive and negative, yield negative changes in the aerodynamic efficiency. The baseline taper ratio produces the best aerodynamic efficiency while keeping the other parameters constant.

The baseline winglet is inclined 90 degrees from the horizontal axis. In this study, the angle was changed by -15 degrees down to 15 degrees. While keeping all of parameters the same and only changing the inclination angle of the baseline winglet, those altered winglets all produced a negative change in aerodynamic efficiency. This seems logical as the effective height of the winglet decreases allowing the generated vortex to curl over the winglet.

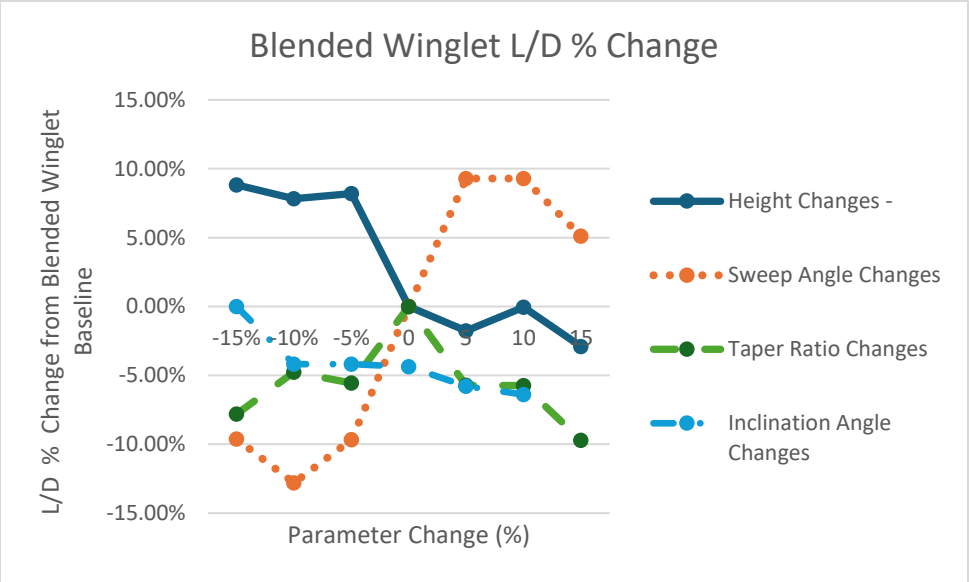

Figure 11. Blended winglet parameter aerodynamic efficiency changes

C. Canted Winglet

Although the B737-700 uses blended winglets, canted winglets are outfitted on the B737-700 3D model extrapolating data found by Scholz [19]. Scholz has the data of the canted winglet used on a B747-400. The canted winglet dimensions are scaled down to 54% of its original size and applied to the B737-700 wing as the wingspan of the B737-700 is 54% of the B747-400. This canted winglet that is extrapolated from the B747-400 yields an aerodynamic efficiency of 3.42 and will act as the baseline for all parameter changes for this winglet type. The boundary conditions used for each for each flow simulation are the same used in the blended winglet flow simulations and can be found in Table 3.

The parameters adjusted for the canted winglet design are found in

Table 5 and include the height, sweep angle, taper ratio and inclination angle. Each parameter is adjusted in 5% increments from the baseline up to +/- 15% except for the inclination angle as the inclination angle is adjusted by 15 degrees from 90 down to 15 degrees.

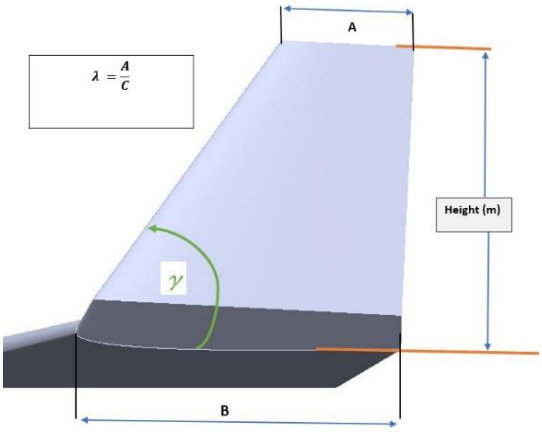

Figure 12. Baseline canted winglet geometry 1

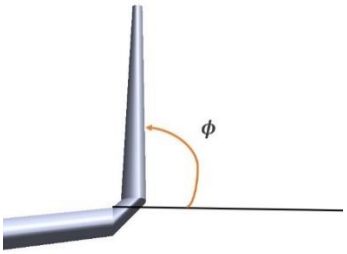

Figure 13. Baseline canted winglet geometry 2

Table 5. Canted winglet design of experiment table

	Parameter	-15%	-10%	-5%	Baseline	+5%	+10%	+15%
Canted Winglet	Height (m)	1.14750	1.12150	1.2875	1.3500	1.4175	1.4850	1.5525
	Sweep Angle (degree)	48.45	51.30	54.15	57.00	59.85	62.7	65.55
	Taper Ratio	0.3825	0.4050	0.4275	0.4500	0.4725	0.4950	0.5175
	Inclination Angle (degree)	15	30	45	90	75	60	-

Table 6. Canted winglet CFD results - L/D output in terms of % change

	Parameter	-15%	-10%	-5%	Baseline	+5%	+10%	+15%
Blended Winglet	Height (m)	-2.90%	-1.34%	-1.44%	L/D = 3.42	-3.35%	-4.05%	-7.48%
	Sweep Angle (degree)	+2.09%	-4.86%	-3.52%		+5.42%	+6.21%	-0.27%
	Taper Ratio	-3.34%	-3.75%	-4.09%		-2.50%	-4.65%	-4.46%
	Inclination Angle (degree)	15 deg	30 deg	45 deg		60 deg	75 deg	-
		+2.75%	+1.8%	+6.97%		+6.19%	+1.79%	

Table 6 displays the aerodynamic efficiencies output for all the parameters that were changed for the baseline canted winglet. The best performing winglets for each parameter are the baseline height, +10% increase in sweep angle, baseline taper ratio, and a 45-degree inclination angle.

Error! Reference source not found.**Figure 11** displays the aerodynamic efficiency changes (L/D) compared to the baseline, the same data found in Table 6. For any positive change in the aerodynamic efficiency, the data point is above the x axis and a negative change will be below the x axis.

For the height changes to the canted winglet baseline, the data shows baseline winglet height yields the best aerodynamic efficiency. Any increase or decrease to the height yields a negative change. The +15% height change for the canted winglet was the worst preforming with a -7.48% change in aerodynamic efficiency when compared to the canted winglet baseline.

The sweep angle changes of the canted winglet from -15% to +15% are studied in this research. The greatest positive change in aerodynamic efficiency comes from the +10% (62.7 deg) in the sweep angle of the baseline canted winglet with a + 6.21%. The sweep angle changes do not follow a trend as the values oscillate from positive to negative and back to positive. The peaks at the + 10% sweep angle change and is the lowest at the – 10% sweep angle change.

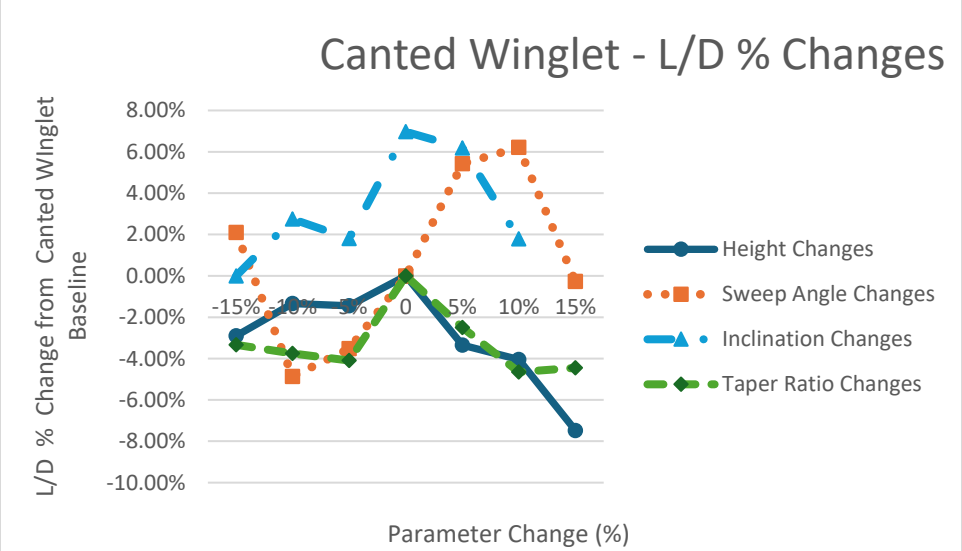

Figure 15. Canted winglet parameter aerodynamic efficiency changes

Next, the taper ratio in this canted winglet let study ranges from 0.3825 to 0.5175. The taper ratio for the baseline, 0.4275, yields the best aerodynamic efficiency. All the changes to the taper ratio change the aerodynamic efficiencies in the negative direction at an average of about -4%.

Finally, this study changes the inclination angle of the canted winglet range

from 90 degrees to 15 degrees in 15-degree increments. All inclination angle changes yield positive aerodynamic efficiency changes. The trend shows an upward trajectory peaking when the canted winglet is at 45 degrees. This change in inclination angle improves the aerodynamic efficiency by + 6.97%.

D. Wingtip Fence Winglet

The wingtip fence is intended to improve the aerodynamic efficiency by

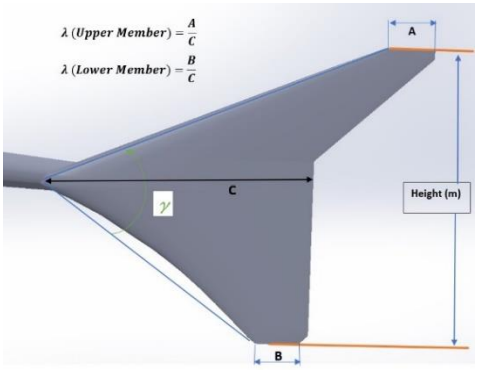

increasing the generated lift at the wingtip and reducing the induced drag caused by wingtip vortices. This type of winglet device is airbus specific and was first introduced in the mid 1980's. The advantage of the wingtip fence is the winglet is shorter than other winglets with similar performances by extending above and below the wing plane. The B737-700 and A319 are very similar aircraft in terms of size, role, and performance. Although this study uses Boeing 737-700 wing as the baseline, the wingtip fence of the Airbus A319 is outfitted to the B737-700 wing.

There are no published engineering drawings of the A319 wingtip fence, so the wingtip fence was reversed engineered to be outfitted to the wing in this study as seen in **Error! Reference source not found.**. The upper and lower members of this winglet have different geometry (sweep angle and taper ratios).

The parameters that are varied from -15% to +15% in 5% increments from the baseline are the height of the winglet, sweep angle and the taper ratios. The height of the wingtip fence winglet is defined as the total length from the upper to the lower member. The sweep angle is defined as the angle of the leading edges of the upper and lower members. The taper ratios of each member vary slightly but each are varied by 5% increments. Looking at

Figure **14**, the taper ratio of upper member is defined as the length of A to the length of C and the taper ratio of the lower member is defined as the length of B to the length of C. Flow simulations were completed in Solidworks with the same boundary conditions as seen in Table 2.

Figure 14. Baseline wingtip fence and geometry

Error! Reference source not found. shows the output aerodynamic efficiency of each parameter change compared to the wingtip fence baseline winglet and wing. The baseline wingtip fence yielded the highest (3.84) aerodynamic efficiency compared to the blended (3.45) and canted (3.42) winglet baselines despite being outfitted to the same wing. All the changes to the height, sweep angle, and taper ratios to the wingtip fence baseline winglet decreased the aerodynamic efficiency.

The height analyzed for the wingtip fence ranged from 1.57 m to 2.12 m. The wingtip fence that performed the best during cruising conditions has the baseline height of 1.85 m. All changes to the height of the winglet decreased the ratio of lift to drag. The

next best aerodynamic efficiency occurred when decreasing the height by -5%. When increasing the height of the wingtip fence, the aerodynamic efficiency decreases between 5% and 7%.

Next, the sweep angles used in this wingtip fence experiment range from 47.88 to 64.78. The baseline wingtip fence winglet performed the best with a 56.33-degree sweep angle. The +10% and +15% change of the sweep angle performed within 1.6% of the baseline.

Again, the best performing wingtip fence in terms of taper ratio is the baseline wingtip. Changing the taper ratio of the upper and lower members decreases the aerodynamic efficiency. This means the reverse engineered geometry of the Airbus A319 is the best preforming wingtip fence in this study.

	Parameter	-15%	-10%	-5%	Baseline	+5%	+10%	+15%
Wingtip Fence Winglet	Height (m)	-2.35 %	-2.39%	-0.35%	L/D = 3.84	-5.34%	-6.36%	-6.29%
	Sweep Angle (degree)	-4.81 %	-5.45%	-1.87%		-2.47%	-0.16%	-1.16%
	Taper Ratio	-2.11 %	-2.30%	-1.41%		-1.23%	-1.01%	-0.92%

Table 8. Wingtip fence winglet CFD results - L/D output in terms of % change

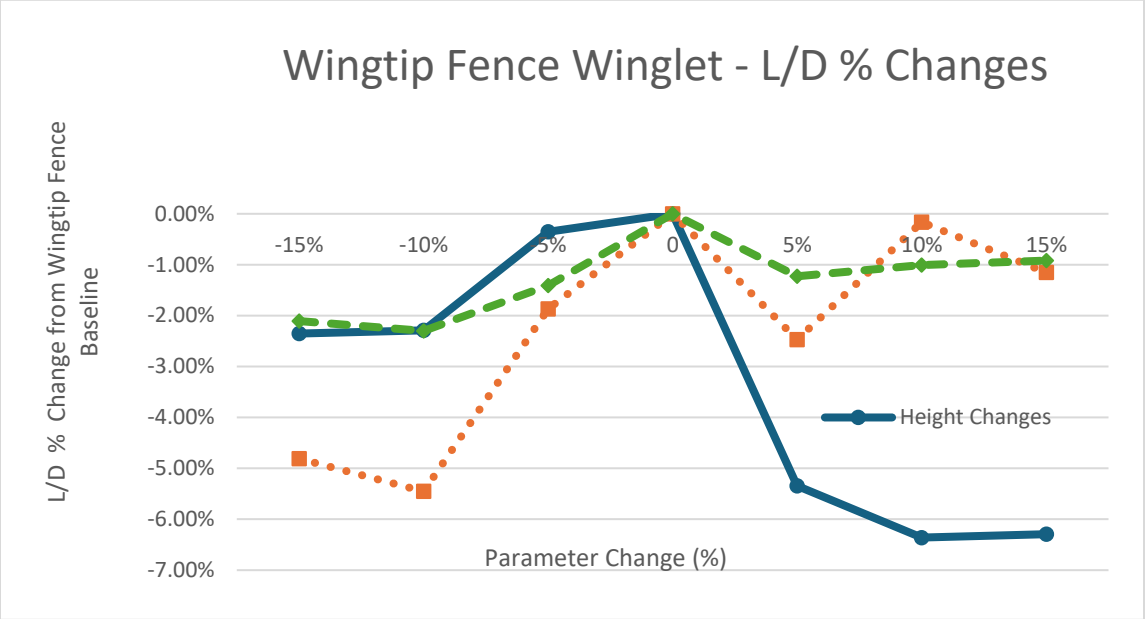

	Parameter		-15%	-10%	-5%	Baseline	+5%	+10%	+15%
Wingtip Fence Winglet	Height (m)		1.57	1.66	1.75	1.85	1.94	2.03	2.12
	Sweep Angle (degree)		47.88	50.68	53.51	56.33	59.15	61.96	64.78
	Taper Ratio	Upper Member	0.168	0.175	0.184	0.194	0.204	0.213	0.223
		Lower Member	0.149	0.158	0.167	0.179	0.185	0.194	0.202

Table 7. Wingtip fence winglet design of experiment table

Figure 15. Wingtip fence winglet parameter aerodynamic efficiency changes

E. Split Scimitar Winglet (SSW)

The split scimitar wing (aka split tip winglet) is an updated and better version of the blended winglet. In addition to the blended winglet, aerodynamicists add a separate member that extends down. This additional member is smaller in geometry but adds an additional blockage to the generated vortex trying to spill over the wing. The split scimitar is the newest type of winglet and is seen on the newest aircraft such as the B737 NG (next generation) family.

Many different aircraft manufactures, and airliners retrofit their aircraft with split scimitar winglet of different sizes. There are no published technical drawings of this type of winglet used on the Boeing 737 NG family, so a winglet was derived. For this experiment, the SSW is derived from the blended winglet used in this experiment with a 15-degree inclination angle. The bottom member is roughly about 1/2 the size of the top member. Multiple models were created with the cord length of the bottom member to understand the effect on aerodynamic efficiency.

The parameters that are varied from -15% to +15% in 5% increments from the baseline are the depth of the bottom member of the winglet, sweep angle and the taper ratio and inclination angle. The depth is measured form the cord line of the wing to the tip of the bottom member as seen in Figure 18. Also shown in Figure 18, is the sweep angle, from the leading edge to the horizonal cord line of the wing. The taper ratio is the ratio of the effective winglet tip length to the length of the base (A/ B in Figure 18). The inclination angle is measured from the horizontal to the plane of the bottom member and is varied by 5-degree increments from -15 to +15 of the baseline values.

Table 9. Split scimitar winglet design of experiment table

	Parameter	-15%	-10%	-5%	Baseline	+5%	+10%	+15%
Split Scimitar Winglet	Depth (m)	1.1568	1.1224	1.2929	1.3610	1.4291	1.4971	1.5652
	Sweep Angle (degree)	37.72	39.94	42.16	44.38	46.59	48.82	51.04
	Taper Ratio	0.1597	0.1691	0.1785	0.1879	0.1972	0.2066	0.2161
	Inclination Angle (degree)	38	43	48	53	58	63	68

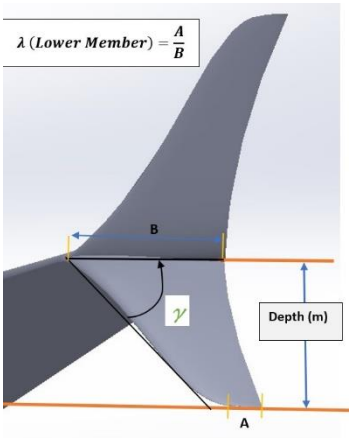

Figure 16. Baseline split scimitar winglet geometry 1

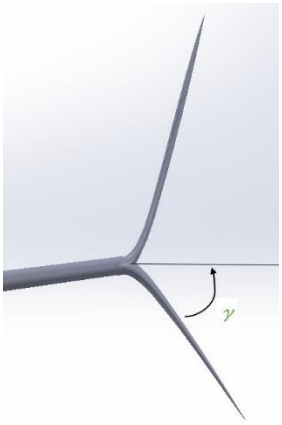

Figure 17. Baseline split scimitar winglet geometry 2

Table 10. Split scimitar winglet CFD results - L/D output in terms of % change

	Parameter	-15%	-10%	-5%	Baseline	+5%	+10%	+15%
Split Scimitar Winglet	Depth (m)	-6.12%	-7.37%	-5.49%	L/D = 3.51	-6.15%	-12.14%	-13.27%
	Sweep Angle (degree)	-4.86%	-7.13%	-6.57%		-8.94%	-8.67%	-9.30%
	Taper Ratio	-9.08%	-8.38%	-7.34%		-7.69%	-8.51%	-8.09%
	Inclination Angle (degree)	38 deg -11.93	43 deg -10.62%	48 deg -6.35%	53 deg	58 deg -6.89%	63 deg -6.87%	68 deg -9.18%

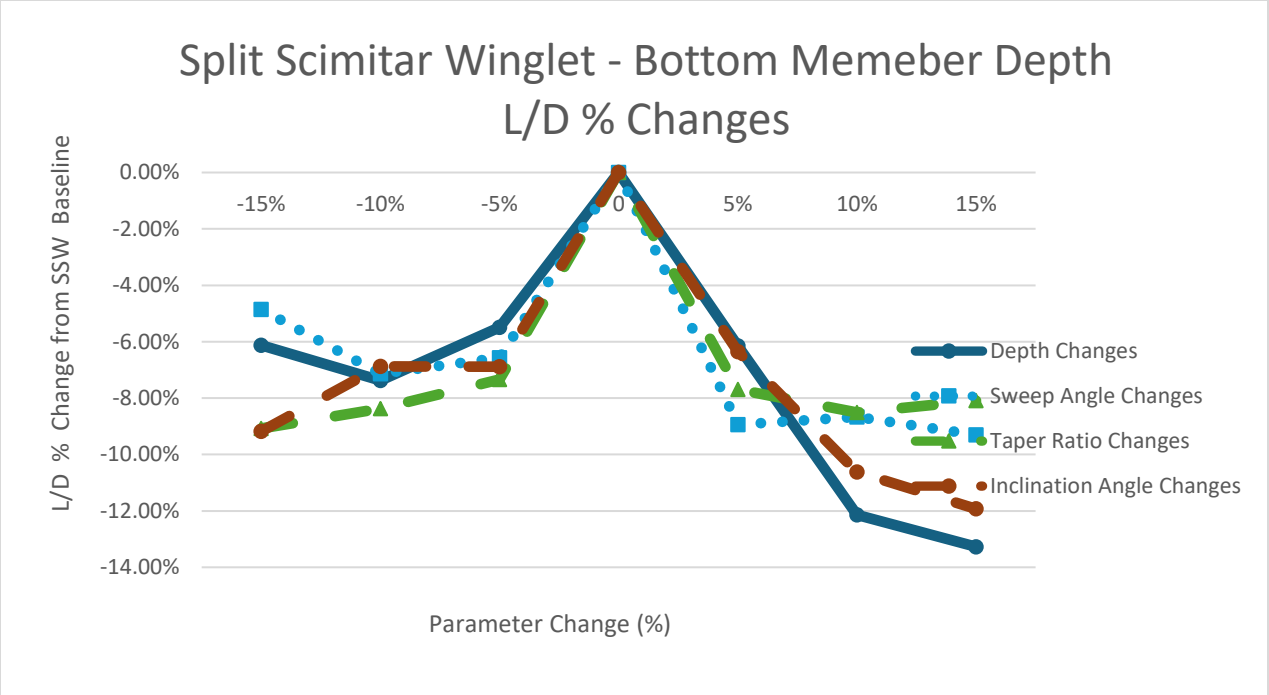

Figure 18. Split scimitar winglet parameter aerodynamic efficiency changes

Table 10 shows the output aerodynamic efficiency of each parameter change compared to the Split Scimitar baseline winglet. The baseline split simitar yielded an aerodynamic efficiency of 3.51. The split scimitar winglet is the blended winglet with an inclination angle of 75 degrees form the horizontal. Adding the bottom member increased the aerodynamic efficiency from 3.31 to 3.51. Compared to the blended (3.45) and canted (3.42) winglet baselines, this is an improvement despite being outfitted to the same wing. All the changes to the height, sweep angle, and taper ratios to the split scimitar baseline winglet decreased the aerodynamic efficiency meaning all the variables were already at their optimum value.

The depth changes analyzed in this study all range from 1.1568 m to 1.5652 m and all yield negative changes of the aerodynamic efficiency to the baseline of 1.3610 m. This means that if the bottom member is made to be shorter than the induced drag due to lift increases, possibly allowing the generated vortex to escape from under the bottom member. Increasing the depth also decreases the aerodynamic efficiency by, possibly increasing the profile drag.

All sweep angle changes also decreased the aerodynamic efficiency of the baseline. The worst preforming sweep angle in the Solidworks Flow Simulation shows a -9.30% to the L/D ratio by increasing the sweep angle by 15%.

The Taper ratio also followed the trend of decreasing the aerodynamic efficiency by increasing or decreasing the

taper ratio of the baseline split scimitar winglet.

The inclination angle is measured from the horizontal to the plane of the bottom member. In this study, the baseline split scimitar winglet has an inclination angle of 53 degrees. By increasing or decreasing this angle, the aerodynamic efficiency decreases under the same boundary conditions.

F. Summary of Computational Fluid Dynamics Results

In Table 11, the aerodynamic efficiencies found in CFD of the OEM winglet of the B737-700, no winglet, and the best performing winglets are displayed. The wing itself with no winglet yields an aerodynamic efficiency of 3.17 at cruise conditions. The aerodynamicists at Boeing were able to increase the aerodynamic efficiency to 3.45 by using a blended winglet, an increase of 21.5% when compared to the wing alone. The OEM winglet is a blended winglet and yields a 3.45 aerodynamic efficiency at cruise conditions. The last column shows the increase in aerodynamic efficiency of the winglet type and its variable changes compared to the OEM B737-700 winglet.

For the blended winglet, the change that best increased the aerodynamic efficiency was increasing the sweep angle by 5%. This yielded a + 9.28% increase from the OEM. For the canted winglet, this was optimized at a 45-degree inclination angle with an increase of +5.80% in aerodynamic efficiency from the OEM winglet. The baseline Wingtip Fence winglet was already optimized and yielded the best aerodynamic efficiency at 3.85, an increase of + 11.59% when compared to the OEM. The Split Scimitar winglet was optimized when the bottom member had the same cord length as the wing itself and a – 15-degree inclination angle. This combination yielded an increase of + 1.74 % to the OEM aerodynamic efficiency.

Table 11. Best performing winglets from CFD analysis

Winglet	Modification	% Modification from Winglet Baseline	L/D	% L/D change from Baseline of Winglet Type	% L/D change from B73-700 OEM Winglet
No winglet	N/A	N/A	3.17	N/A	- 8.70%
B737-700 OEM Blended Winglet	OEM/ Baseline	OEM/ Baseline	3.45	-	-
Blended Winglet (Optimized)	Sweep Angle	+ 5%	3.77	+ 9.28%	+ 9.28%
Canted Winglet	Inclination Angle	-45 deg	3.65	+ 6.73%	+ 5.80%
Wingtip Fence Winglet	Baseline	Baseline	3.85	Baseline	+ 11.59%
Split Scimitar Winglet	Baseline	Baseline	3.51	Baseline	+ 1.74%

VII. 3D PRINTING

The models will be scaled down and 3D printed to be tested in a wind tunnel. The models that will be printed are the wing with no winglet, OEM blended winglet, and the best performing winglet of the blended, canted, wingtip fence and split scimitar. These 6 models will be scaled down to a scale of 4.67%. This scale ensures proper and maximizes fit in the test section of the wind tunnel.

The printer used for this project is a Stratasys F170 with dissolvable support material capabilities as seen in Figure 20-A. The printer uses a different type of filament for the support material. Each print takes about 10 hours, this process includes heating up the cabin of the Stratasys and the print time. This material is dissolved in a Support Cleaning Apparatus seen in **Figure 19** . The

apparatus is filled with a solution and heats up to 80 degrees Celsius to dissolve the support material over an 8-hour process.

Figure 19. Support cleaning apparatus

Figure 20. Stratasys F170 3D printer

Each winglet print takes between 10-11 hours to complete. The way these parts are arranged on the print bed are that the leading edge of the wing is touching the bed so that the leading edge would the last layer printed as these are the thinnest areas of the part.

The prints did not come out perfectly as the last layer is so thin and the filament struggles to stick. After the bath and touch ups with sandpaper, the parts and the interactions between the winglet and wing are smooth, the parts are ready for the wing tunnel.

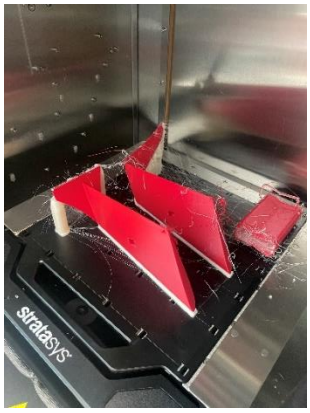

Figure 21. Blended winglet & wingtip fence print

Figure 22. Split scimitar winglet 3D print

VIII. WIND TUNNEL TESTING

A. Experimental Setup

An Educational Wind Tunnel (EWT) is used to analyze the aerodynamic performance of the 3D printed winglets. A probe reads the axial (drag) and normal (lift) forces. The EWT can reach speeds of up to 120 mph. For this experiment, a limit of about 50 mph is set for the safety of the equipment. This limit does not allow for Reynold's number to be matched to the CFD testing. Testing the performance of each winglet includes running the wind tunnel at 10-40% of its maximum speed at 5%

increments and at pitch angles of –5 degrees to 15 degrees in 5-degree increments.

Another aspect that limited the wind tunnel testing is due to the asymmetric winglets. At higher speeds, the wing and winglet would generate lift, but it would not be balanced around the point of center of gravity. This imbalance would cause the whole print to rotate around the probe. To counteract this issue, a small foam block was fixed to the backside of the print. This foam block did solve the issue of the print rotating but did not allow the axial force to be registered correctly. The wind tunnel testing for this experiment only considers the lift generated by the winglet.

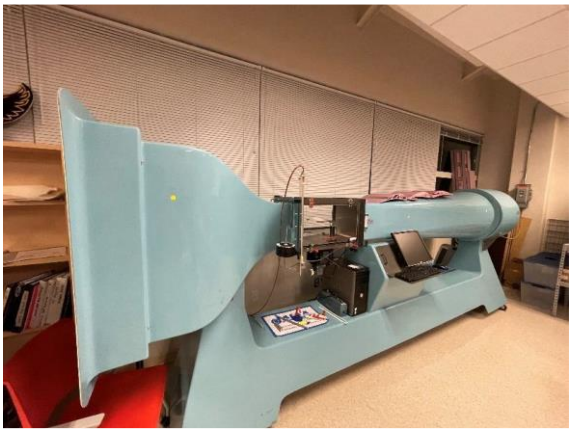

Figure 23. Educational wind tunnel

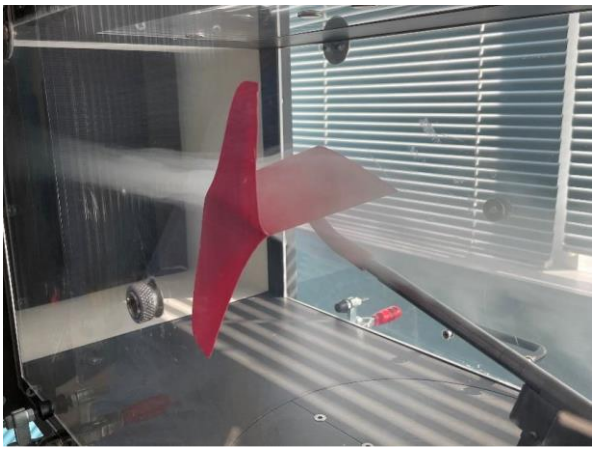

Figure 24. Wind tunnel testing of SSW

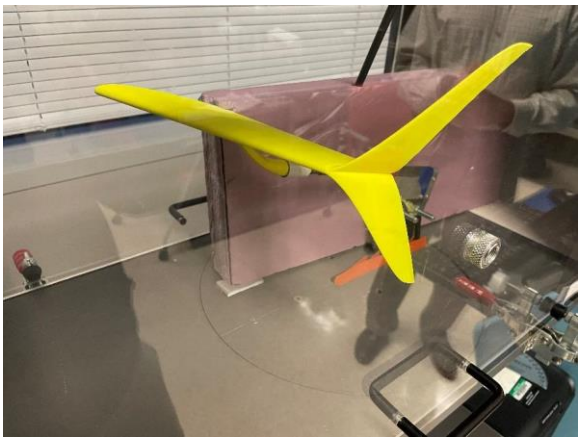

Figure 25. Wind tunnel experimental setup

B. No Winglet Wind Tunnel Test Results

The results depicted in Table 13 show that the wing without a winglet yields the highest lift value at a pitch angle of 15 degrees and 40% of the maximum speed of the wind tunnel. The value reached is 0.35 lbf of lift with an extreme angle of attack at the maximum speed allowed for the experiment.

Table 12. No winglet - wind tunnel testing lift results (lbf)

Speed %	Angle of Attack				
	-5 degrees	0 degrees	5 degrees	10 degrees	15 degrees
10	0	0	0.01	0.01	0.01
15	-0.01	0	0.03	0.04	0.04
20	-0.03	0	0.05	0.09	0.07
25	-0.05	0	0.09	0.13	0.13
30	-0.07	0.01	0.15	0.19	0.19
35	-0.11	0.02	0.19	0.25	0.25
40	-0.15	0.04	0.26	0.32	0.35

C. OEM Winglet Wind Tunnel Test Results

In Table 14, the maximum lift reached is 0.45 lbf at a 10-degree pitch angle and at 40% speed. This means that a larger lift value was reached at a shallower pitch angle with the OEM winglet compared to the test with no winglet.

Table 13. OEM winglet - wind tunnel testing lift results (lbf)

Speed %	Angle of Attack				
	-5 degrees	0 degrees	5 degrees	10 degrees	15 degrees
10	0	0	0.03	0.03	0
15	-0.01	0	0.05	0.07	0.03
20	-0.03	0	0.08	0.12	0.03
25	-0.05	0.01	0.11	0.19	0.10
30	-0.09	0.02	0.17	0.25	0.2
35	-0.13	0.04	0.26	0.35	0.28
40	-0.18	0.06	0.33	0.45	0.36

D. Blended Winglet Wind Tunnel Test Results

The optimized blended winglet wind tunnel testing results are shown in Table 15, and the largest lift value of 0.48 lbf is obtained at a 5-degree pitch angle at maximum testing speed. The optimized blended winglet has a slightly larger lift value than the OEM blended winglet but at a shallower pitch angle.

Table 14. Blended winglet - wind tunnel testing lift results (lbf)

Speed %	Angle of Attack				
	-5 degrees	0 degrees	5 degrees	10 degrees	15 degrees
10	-0.01	0	0.01	0.02	0.01
15	-0.02	0	0.06	0.04	0.04
20	-0.03	0.01	0.09	0.07	0.08
25	-0.06	0.02	0.13	0.14	0.15
30	-0.09	0.05	0.23	0.19	0.21
35	-0.13	0.07	0.34	0.26	0.28
40	-0.19	0.08	0.48	0.38	0.37

E. Canted Winglet Wind Tunnel Test Results

In Table 16, the results of the canted winglet wind tunnel testing indicated the largest value of lift, 0.63 lbf, was obtained at a 15-degree pitch angle and at maximum speed of the experiment. This is the largest value of lift obtained in the entire wind tunnel testing.

Table 15. Canted winglet - wind tunnel testing lift results (lbf)

Speed %	Angle of Attack				
	-5 degrees	0 degrees	5 degrees	10 degrees	15 degrees
10	-0.01	0	0.01	0.04	0
15	-0.03	0	0.05	0.09	0.02
20	-0.05	0	0.09	0.14	0.16
25	-0.08	0.01	0.15	0.20	0.27
30	-0.12	0.01	0.23	0.32	0.35
35	-0.18	0.03	0.33	0.42	0.48
40	-0.28	0.04	0.47	0.54	0.63

F. Wingtip Fence Winglet Wind Tunnel Test Results

In Table 17, the largest value of lift obtained by the wingtip fence winglet in wind tunnel testing is only 0.37 lbf. This value is obtained at maximum speed at a degree pitch angle. During CFD tests, the wingtip fence improved the aerodynamic efficiency the most but the wind tunnel testing indicates only slightly more lift.

Table 16. Wingtip fence winglet - wind tunnel testing lift results (lbf)

Speed %	Angle of Attack				
	-5 degrees	0 degrees	5 degrees	10 degrees	15 degrees
10	-0.01	001	0	0.01	0
15	-0.02	0.01	0.02	0.04	0.02
20	-0.04	0.01	0.03	0.08	0.04
25	-0.06	0.01	0.05	0.14	0.07
30	-0.09	0.01	0.10	0.2	0.15
35	-0.13	0.02	0.18	0.26	0.22
40	-0.18	0.04	0.24	0.37	0.31

G. Split Scimitar Winglet Wind Tunnel Test Results

In Table 18, the largest value of lift, 0.59 lbf, for the wind tunnel testing of the Split Scimitar winglet is obtained at maximum speed of the experiment and a 15-degree pitch angle. This is the second largest

value of lift obtained in the wind tunnel testing portion of this study.

Table 17. Split scimitar winglet - wind tunnel testing lift results (lbf)

Speed %	Angle of Attack				
	-5 degrees	0 degrees	5 degrees	10 degrees	15 degrees
10	0	0	0.03	0	0.02
15	-0.01	0	0.05	0.03	0.06
20	-0.03	0	0.07	0.09	0.13
25	-0.06	0.02	0.15	0.17	0.22
30	-0.10	0.03	0.24	0.26	0.31
35	-0.14	0.06	0.35	0.40	0.45
40	-0.19	0.12	0.50	0.53	0.59

IX. CONCLUSION

In conclusion, the CFD results indicate that the wing tip fence is the most aerodynamically efficient winglet while wind tunnel results indicate that the canted winglet produced the largest lift value. These analyses indicate that the geometric changes for each type of winglet could improve the aerodynamic performance of the wings compared to their original design. The wind tunnel tests for the best of each type of winglet indicate that the results matched with those obtained from physics-based models and CFD analyses. Since the wind tunnel testing is limited due to the asymmetric nature of the 3D prints, only the values of lift are analyzed. All these values are improvements upon the OEM winglet found on the B737-700. This extensive research on winglet performance indicates that the potential cost savings are large and could affect many aircraft designs, manufacturers, airlines, and people.

X. REFERENCES

[1] M. Johnston, “A beginner's guide to airplane winglets - Calaero University,” California Aeronautical University. https://calaero.edu/guide-airplane-winglets/.

[2] N. Cummins, “Why Boeing has winglets and Airbus has sharklets,” Simple Flying. https://simpleflying.com/boeing-winglets-airbus-sharklets/.

[3] S. Merryisha and P. Rajendran, “Review of winglets on tip vortex, drag and airfoil geometry,” Journal of Advanced Research in Fluid Mechanics and Thermal Sciences, vol. 63, no. 2, Dec. 2020.

[4] M. Azlin, C. Mar Talib, S. Kasolang, and F. Muhammad, “CFD analysis of winglets at low subsonic flow,” Proceedings of the World Congress on Engineering, vol. 1, Jul. 2011.

[5] B.S. de Mattos, P. Komatsu, and J. Tomita, “Optimal wingtip device design for transport airplane,” *Aircraft Engineering and Aerospace Technology*, vol. 90, no. 5, Aug. 2018.

[6] A. Al-Mahadin and M. Almajali, "Simplified mathematical modelling of wing tip vortices," Advances in Science and Engineering Technology International Conferences (ASET), 2019, pp. 1-6, doi: 10.1109/ICASET.2019.8714214.

[7] D. Heathers., “New Boeing 777 raked wing tips improve fuel efficiency, good for the environment,” MediaRoom. https://boeing.mediaroom.com/2002-10-01-New-Boeing-777-Raked-Wing-Tips-Improve-Fuel-Efficiency-Good-for-the-Environment.

[8] C. Brady, "Detailed technical data," The Boeing 737 Technical Site. http://www.b737.org.uk/techspecsdetailed.htm.

[9] G. Narayan and B. John, "Effect of winglets induced tip vortex structure on the performance of subsonic wings," *Aerospace Science and Technology*, vol. 58, no. 1, pp. 328–340, Sep. 2016.

[10] J. Crowe, F. Ramos, C. Fricks, E. Cathers, and E. Pernell, "Analysis of various blended winglet additions to Cessna 172, Piper Malibu, and Boeing 737 wings," thesis, Allen E. Paulson College of Engineering and Computing, Statsboro, 2021.

[11] A. Al-Khafaji , G. Panatov, and A. Boldyrev, Research Square, Rostov-on-Don, Russia, tech., 2021.

[12] P. Gehlert, K. Sabnis, and H. Babinsky, "Effect of winglet serration geometry on the wingtip vortex," AIAA SCITECH 2022 Forum, Jan. 2022.

[13] Z. Hui, G. Cheng, and G. Chen, "Experimental investigation on tip-vortex flow characteristics of novel bionic multi-tip winglet configurations," *Physics of Fluids*, vol. 33, no. 1, pp. 1–16, Jan. 2021.

[14] R. C. Hibbeler, Fluid mechanics, NY, New York: Pearson, 2018.

[15] D. P. Raymer, *Aircraft design: A conceptual approach*, Blacksburg, Virginia: American Institute of Aeronautics and Astronautics, 2021.

[16] J. Jewell, C. Soret, P. Bradley, and T. Almahmood, "CFM56-7: An in-depth look at the new industry leader," *CFM International*. https://www.cfmaeroengines.com/press-articles/cfm56-7-an-in-depth-look-at-the-new-industry-leader/.

[17] "Airfoil tools," Airfoil Tools. http://www.airfoiltools.com/.

[18] "UIUC applied Aerodynamics Group," UIUC Applied Aerodynamics Group. https://m-selig.ae.illinois.edu/.

[19] D. Scholz, "Definition and discussion of the intrinsic efficiency of winglets," *INCAS Bulletin*, vol. 10, no. 1, pp. 117–134, Mar. 2018. doi: 10.13111/2066-8201.2018.10.1.12.